

# Simulation of the Effects of the Preceding SST Anomalies over the Tropical Eastern Pacific on Precipitation to the South of the Yangtze River in June\*

LI Yan<sup>1,2</sup>(李 琰), WANG Yafei<sup>1†</sup>(王亚非), and DONG Min<sup>3</sup>(董 敏)

<sup>1</sup> State Key Laboratory of Severe Weather, Chinese Academy of Meteorological Sciences, Beijing 100081

<sup>2</sup> Nanjing University of Information Science & Technology, Nanjing 210044

<sup>3</sup> Laboratory for Climate Studies, National Climate Center, China Meteorological Administration, Beijing 100081

(Received January 12, 2009)

## ABSTRACT

Numerical experiments are performed to simulate the response of the atmospheric circulation and precipitation over East China in June to the sea surface temperature (SST) anomalies over the tropical eastern Pacific (TEP) from preceding September to June by using an atmospheric general circulation model (AGCM). We constructed composite positive/negative SST anomalies (P-SSTAs/N-SSTAs) based on the observational SST anomalies over the TEP from September 1997 to June 1998. The results show that: (1) the response of the precipitation in the Yangtze River basin and its southern area (YRBS) to El Niño with different durations varies with the maximum amplitude of the precipitation anomalies appearing when the imposed duration is from November to next June, and the minimum appearing when the SST anomalies is only imposed in June. The anomalies of the precipitation are reduced when the duration of the forcing SST anomalies over the TEP is shortened and the positive SST anomalies in the preceding autumn tend to cause significantly more rainfall in the YRBS. This is in agreement with previous diagnostic analysis results. (2) The simulated precipitation anomalies over the YRBS are always obviously positive under strong or weak positive SST anomalies over the TEP. The intensity of the precipitation anomalies increases with increasing intensity of the SST anomalies in the experiments. The simulation results are consistent with the observations during the warm SST events, suggesting reasonable modeling results. (3) When negative SST anomalies in the TEP are put into the model, the results are different from those of the diagnostic analysis of La Niña events. Negative precipitation anomalies in YRBS could be reproduced only when the negative SST anomalies are strong enough.

**Key words:** atmospheric general circulation model (AGCM), sea surface temperature (SST) anomalies, numerical simulation

**Citation:** Li Yan, Wang Yafei, and Dong Min, 2009: Simulation of the effects of the preceding SST anomalies over the tropical eastern Pacific on precipitation to the south of the Yangtze River in June. *Acta Meteor. Sinica*, **23**(6), 691–700.

## 1. Introduction

The global climate change is attributable to many reasons such as the variation of the Indian Ocean sea surface temperature (SST), El Niño-Southern Oscillation (ENSO), snow cover, etc., among which ENSO is an essential factor as pointed out by Namias (1959). Most of scientists have focused on understanding the influence of SST anomalies over the tropical eastern Pacific (TEP). Specific attention has been paid to the

forcing of SST anomalies on the local and remote precipitation (Rasmusson and Wallace, 1983; Yulaeva and Wallace, 1994; Wu and Wang, 1996). Scientists found that the SST anomalies over the TEP play an important role in the precipitation in the mid-low reaches of the Yangtze River in summer (Luo et al., 1985; Miao et al., 2002). Chinese meteorologists also found that there was a noticeable relationship between El Niño and precipitation over East China in the ensuing summer. When an El Niño event occurred, there would

\*Supported by the National Natural Science Foundation of China under Grant No. 40675034, China-Japan intergovernmental cooperation program of the Japan International Cooperation Agency under Grant No. 2009LASWZF04, the program of Ministry of Science and Technology of China under Grant No. 2009DFB20540, and the Science and Technology Innovation Program of Jiangsu Province under Grant No. CX09B-221Z.

†Corresponding author: yfwang@cams.cma.gov.cn.

be more precipitation in the mid-to-low reaches of the Yangtze River and less precipitation over North China (the Long-Range Weather Forecasting Group of Institute of Atmospheric Physics, 1978). Wang et al. (2001) and Wang and Fujiyoshi (2004) found that the Nino3 SST in the preceding fall has significant positive correlations with the summer geopotential height in the subtropical regions of East Asia, the western North Pacific, and Northeast Asia. A strong (weak) summer monsoon in the subtropical regions of East Asia tends to occur about two to three seasons after the Nino3 SST anomalies exceeding  $1.5^{\circ}\text{C}$  (dropping to  $-0.7^{\circ}\text{C}$ ). The results suggest a delayed impact of ENSO on the East Asian summer atmospheric circulation. In our earlier work (Li et al., 2007), the relationship between the SST anomalies over the TEP and the precipitation over the Yangtze River basin and its southern area (YRBS) in June, July, and August was examined respectively by using observational data. The most significant correlation over the YRBS occurred in June. This conclusion coincides with the results of Wang et al. (2001).

On the other hand, the Atmospheric General Circulation Model (AGCM) of National Center for Atmospheric Research (NCAR) are used broadly in simulating the atmospheric circulation and estimating the response of the climate change as well as the effects of human activities on climate. Many studies on the response of the atmospheric circulation to SST anomalies indicated that the AGCM of NCAR could preferably describe the large-scale climate characteristics in East Asia, especially the atmospheric response to SST anomalies (Dong, 1997; Xu et al., 2001; Chen et al., 2002; Yuan et al., 2004; Wang and Qian, 2005; Li et al., 2006).

Based on the previous works mentioned above, we will address the relationships between the anomalous precipitation over the YRBS in June and the SSTA in the TEP by using the NCAR Community Atmosphere Model Version 3.0 (CAM3.0). A series of sensitivity experiments were conducted to evaluate the impact of SST anomalies on the precipitation over the YRBS in June.

## 2. Model description and experimental design

### 2.1 Model description

The CAM3.0 adopts  $\eta$ -coordinate and 26 vertical layers. The nonlinear terms and the parameterized physical processes are calculated on a  $128 \times 64$  Gaussian grid with a horizontal resolution of about  $2.8125^{\circ} \times 2.8125^{\circ}$ . The time integral adopts the semi-implicit scheme with a time step of 20 min. The model includes full physical processes such as radiation, cloud, convection, land surface, boundary layer, etc. More details can be found in the model description document (Collins et al., 2004).

The model includes two optional ocean models: one drives the atmosphere model by taking monthly mean SST as a boundary field, called Data Ocean Model (DOM), and the other runs in coupling with a simple ocean model called Slab Ocean Model (SOM). The two operational ways include ocean, land, and air, composing an integrated land-air system. We adopted the DOM in our experiments. A seasonally varying SST and sea-ice concentration dataset is used to prescribe the time evolution of these surface quantities. This dataset prescribes climatological monthly mid-point mean values of SST and ice concentration. The SST and sea ice concentrations are updated every time step by the model at each grid point using linear interpolation in time. In our work, we merely consider the impact of the SST anomalies on the atmosphere without considering the feedback of the atmosphere to ocean.

### 2.2 Experimental design

A set of experiments is performed to investigate the impacts of preceding SST anomalies over the TEP on the precipitation anomalies over the YRBS.

(1) Control experiment. The climatological SST is taken as one of the boundary fields and the model is integrated for 20 yr, in which the mean of the last 5 years was regarded as a model climate.

(2) The first series of sensitivity experiments (SEXP1). Since this study focused on the El Niño

events, realistic SST anomalies in the TEP from September 1997 to June 1998 were put into the model, and this suite of experiment was called P-SSTA. The P-SSTA fields with 10 different durations, i.e., from September to June, from October to June, from May to June, and in June, were imposed over the TEP respectively with seasonally varying climatological SST over the rest of the area. Sensitive experiments were performed for the above durations respectively. The purpose of SEXP1 was to study the impacts of the preceding autumn SST anomalies over the TEP on the atmospheric circulation and precipitation over the YRBS in June. The spatial distribution of the SST anomalies in preceding September was shown in Fig. 1. The maximum imposed anomalies are  $3.7^{\circ}\text{C}$  which are comparable to values in the mature phase of the 1997/1998 El Niño. The spatial pattern of the SST anomalies in the following months are similar to that in September shown in Fig. 1 and the values of the following months are reduced correspondingly based on that during 1997/1998.

(3) The second series of sensitivity experiments (SEXP2). In order to study the stability and sensitivity of the simulation results, we simulated the precipitation anomalies responding to various intensity P-SSTAs from September 1997 to June 1998. Based on the SST anomalies prescribed in the SEXP1, the SST anomalies were modified by adding or subtracting  $0.5^{\circ}\text{C}$  at all grid points. The sensitivity exper-

iments were conducted to simulate the precipitation response to the intensity of SST anomalies persistent from September 1997 to June 1998. These experiments were referred to as SEXP2-P1, SEXP2-P2, SEXP2-P3, SEXP2-P4, and SEXP2-P5, respectively, which were named in terms of the maximum SST, i.e.,  $2.7$ ,  $3.2$ ,  $3.7$ ,  $4.2$ , and  $4.7^{\circ}\text{C}$ .

Similarly, the negative SSTA (N-SSTA) experiments have the same magnitude as those in the SEXP2-P1, ..., SEXP2-P5 except with negative signs. The experiments were integrated from 1 September 1997 to 30 June 1998 to simulate the precipitation response to various intensity N-SSTAs, which are referred to as SEXP2-N1, ..., SEXP2-N5.

For each of the above forcing scenarios, the prescribed SST anomalies were added to the monthly mean climatological SST field without the change of other parameters. The last 5 years of the 20-yr integrations of the control experiment were used to construct a 5-member ensemble mean to reduce the nonlinear errors caused by differing initial conditions. The average result of the five integrations was taken as the result of the sensitivity experiments. The atmospheric circulation and precipitation anomalies from the sensitivity experiments were obtained by subtracting the control experiment from the sensitivity experiments.

### 2.3 Data

In order to assess the model ability to simulate

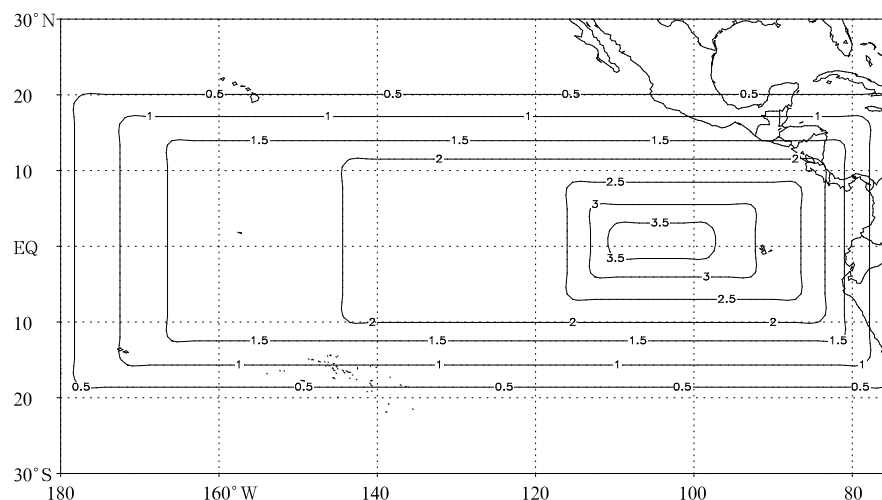
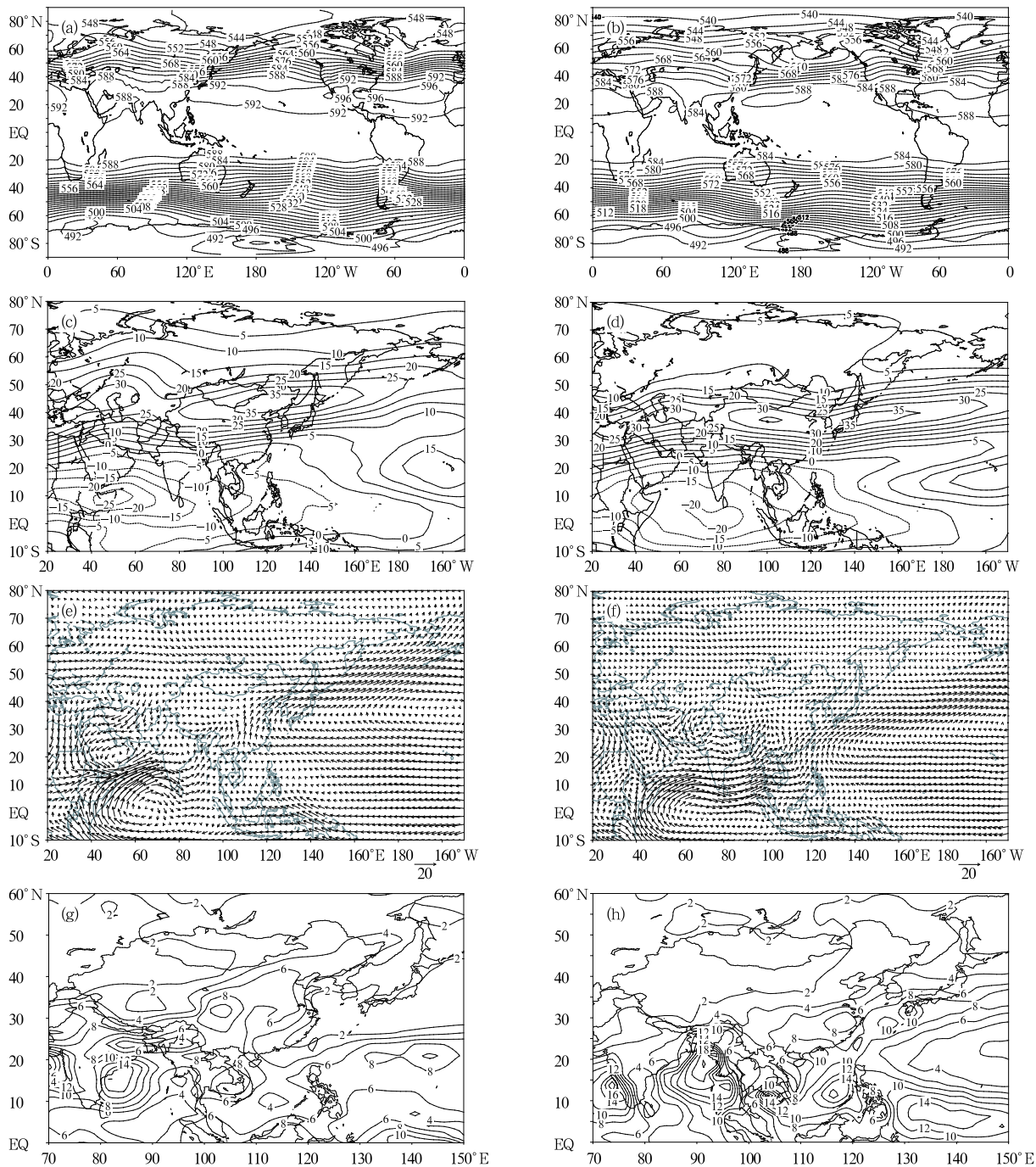


Fig. 1. A sketch map of positive SST anomalies ( $^{\circ}\text{C}$ ) in September over the TEP.



**Fig. 2.** Mean climate of June based on the model simulation (left panels) and NCEP/NCAR reanalysis (right panels). (a) and (b) 500-hPa geopotential height (gpm); (c) and (d) 200-hPa wind field ( $\text{m s}^{-1}$ ); (e) and (f) 850-hPa wind vector in ( $\text{m s}^{-1}$ ); and (g) and (h) precipitation ( $\text{mm day}^{-1}$ ).

the Asian monsoon and precipitation, the NCEP/NCAR reanalysis data were used for comparison. NCEP reanalysis data provide monthly 200-hPa wind, 850-hPa wind, and 500-hPa geopotential height

fields with a horizontal resolution of  $2.5^\circ$ , covering a 50-yr period from January 1951 to December 2000. For more details, please refer to the data description documents (Kalnay et al., 1996; Su et al., 1999).

### 3. Experiment results

#### 3.1 Results of the control experiment

The control experiment is carried out with seasonally varying climatological SST as a lower boundary condition and it is initialized from climatological fields.

Figure 2 shows that the model simulates the pattern of observational geopotential height at 500 hPa (Z500) quite well (Fig. 2a). But there are some deficiencies, especially the amplitude of the model simulation, which is somewhat higher than the observation shown in Fig. 2b by about 4 gpm. The simulated western Pacific subtropical high extends westward further about 10 longitudes along 30°N compared with the observation. The simulated deep trough of East Asia stretches westward by 20 longitudes compared with the observation located around 150°E originally. The simulated westerly jet and easterly jet shown in Fig. 2c are located along 40°N and 10°N, respectively, coinciding with those in the observation (Fig. 2d). But the simulated maximum center of the westerly jet lies at (40°N, 120°E) which is farther northwestward compared with the observation. The maximum center of the easterly jet which lies at (10°N, 50°E) is also northwestward compared with the observation. The Somalia equatorial jet, the southwesterly over the Indian Ocean and the southeasterly along the East Asian coast at 850 hPa are roughly reproduced (Fig. 2e). The simulations can describe major features of the June precipitation in China, i.e., more precipitation in the south and less precipitation in the north (Fig. 2g). The simulated maximum center is at 15°N, 85°E, and is about 14 mm day<sup>-1</sup>, which is weaker than that in the observation (Fig. 2h). The other maximum center over the mid-to-low reaches of the Yangtze River valley is not reproduced. In most AGCMs, the rainband over the mid-to-low reaches of the Yangtze River valley is poorly simulated. Many researchers supposed that the differences between the simulated and observed precipitation were due to meso- and small-scale weather processes and the inefficient physical parameterizations, particularly the convective parameterization.

The simulated monthly monsoon circulation and

precipitation are compared with the observations. The results show that the model can capture the main features of the spatial distribution and reproduce the basic pattern of precipitation in China. Thus, we make sensitivity experiments using CAM3.0 to study the effect of SST anomalies over the TEP on the precipitation over the YRBS in June. The differences between the sensitivity experiments and control experiment are used to represent precipitation responding to the SST anomalies over the TEP. The aim of this study is to identify and reduce the systematic biases of the model.

#### 3.2 Sensitive experiment (SEXP1): Impacts of different SST anomaly durations on precipitation in the YRBS

According to our earlier work (Li et al., 2007), the Nino3 index in the preceding autumn and anomalous precipitation in June is significantly correlated over the area (25°–30°N, 110°–120°E). Thus, the area-averaged anomalous precipitation is used to represent the impact of El Niño on rainfall over the whole YRBS. The precipitation anomalies over the YRBS in June result from the effect of positive SST anomalies with different durations are shown in Fig. 3.

The anomalous precipitation has a decreased trend with reduced durations of imposed SST anomalies over the TEP. The maximum is 1.5 mm day<sup>-1</sup> when the imposed duration is from November to next June and the minimum is just 0.137 mm day<sup>-1</sup> when the SST anomalies are only imposed in June. The result shows that strong positive SST anomalies over the TEP in preceding autumn could significantly cause positive precipitation anomalies over the YRBS in June, which provides a delayed impact of SST anomalies on the precipitation in June over the YRBS. This result coincides with the previous diagnostic analyses (Li et al., 2007; Wang et al., 2001, Wang and Fujiyoshi, 2004). The weakest precipitation anomalies shown in Fig. 3 are likely due to the negative SST anomalies over the TEP in June (figure omitted) which is at the decay phase of El Niño. Larger precipitation anomalies over the YRBS tend to occur when the SST anomalies over the TEP from April to June or from May to June are imposed, while smaller precipitation anomalies over the YRBS tend to be associated with

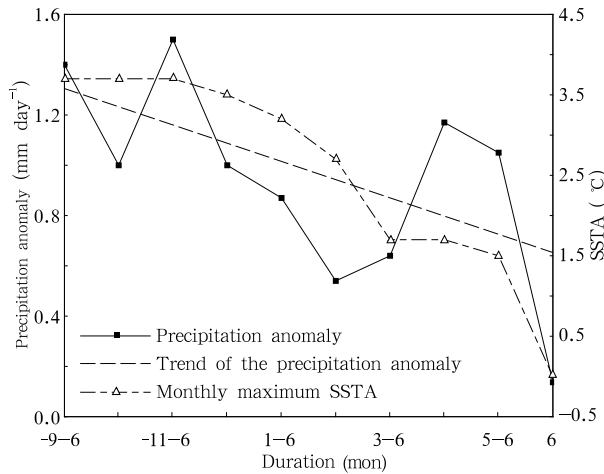


**Fig. 3.** Precipitation anomalies over the YRBS in June resulted from the effect of input positive SST anomalies with different durations. The  $x$  axis shows the SST anomaly durations from preceding September to June, (-9-6), from preceding November to June (-11-6), ..., from May to June (5-6) and only in June (6) respectively.

the SST anomalies over the TEP from February to June or March to June in the model. The results indicate that the SST anomalies from May to June and only in June over the TEP can cause more precipitation in June over the YRBS.

### 3.3 Sensitivity experiment (SEXP2): Impacts of different SST anomaly intensities on precipitation over the YRBS in June

The distributions of precipitation anomalies of experiments SEXP2-P and SEXP2-N are shown in Fig. 4. The area-averaged precipitation anomalies represent the impact of various intensity El Niño (Fig. 5a) and La Niña (Fig. 5b) on the precipitation anomalies over the YRBS in June. The results shown in Figs. 4 and 5 indicate that there are always obvious positive precipitation anomalies over the YRBS in June when strong or weak SST anomalies are imposed over the TEP from September to June. The intensity of the precipitation anomalies increases with that of the SST anomalies imposed. When the N-SSTAs are put into the model, the simulated results are different from the observational impact of La Niña events. Negative precipitation anomalies could be reproduced only when the negative SST anomalies are intensive

enough. These phenomena are also similar to that in the research of the effects of SST anomalies off the east coast of Japan on the development of the Okhotsk high (Wei and Wang, 2006). We suppose that the phenomena maybe due to the model deficiencies or some other factors contributing to the negative precipitation anomalies over the YRBS in June, such as the Atlantic Ocean circulation (Chang et al., 2001). The effect of La Niña on precipitation in June needs to be further clarified.

In summary, there is positive anomalous precipitation over the YRBS in June under strong or weak SST anomalies imposed. The result suggests that the model is sensitive to the SST anomalies over the TEP and the simulated results are stable. Thus, it is believable that the El Niño event in preceding autumn has a delayed impact on the precipitation anomalies over the YRBS in June.

Taking the sensitivity experiments SEXP2-P3 and SEXP2-N3 for example, we examine the response of the atmospheric circulation and precipitation anomalies to El Niño and La Niña respectively in detail. The 500-hPa height anomalies (Z500A) are shown in Fig. 6a. The positive anomaly center is located at 65°N, 160°E and two negative ones are near east coast of Japan and 50°N, 60°E, respectively. The distribution of the two negative Z500A centers and the positive Z500A center is favorable for increased precipitation in June over the YRBS (Wang, 1992; Zhang and Tao, 1998). A major anticyclone circulation anomaly is centered at the Philippine Sea shown in Fig. 6c. The 850-hPa low-level anticyclone circulation anomaly causes anomalously wet conditions along the East Asia and benefits to the increase of precipitation over the YRBS in June. Southwesterly anomalies dominate South China in Fig. 6c, which intensifies the Asian summer monsoon. Pronounced positive precipitation anomalies are over the YRBS in June and the positive anomaly center is located to the north of Jiangxi Province of China as shown in Fig. 4. The distribution of Z500A, 850-hPa anomalous wind, and the precipitation anomalies well agree with the observational distributions in situ (Li et al., 2007).

However, in experiment SEXP2-N3, the positive

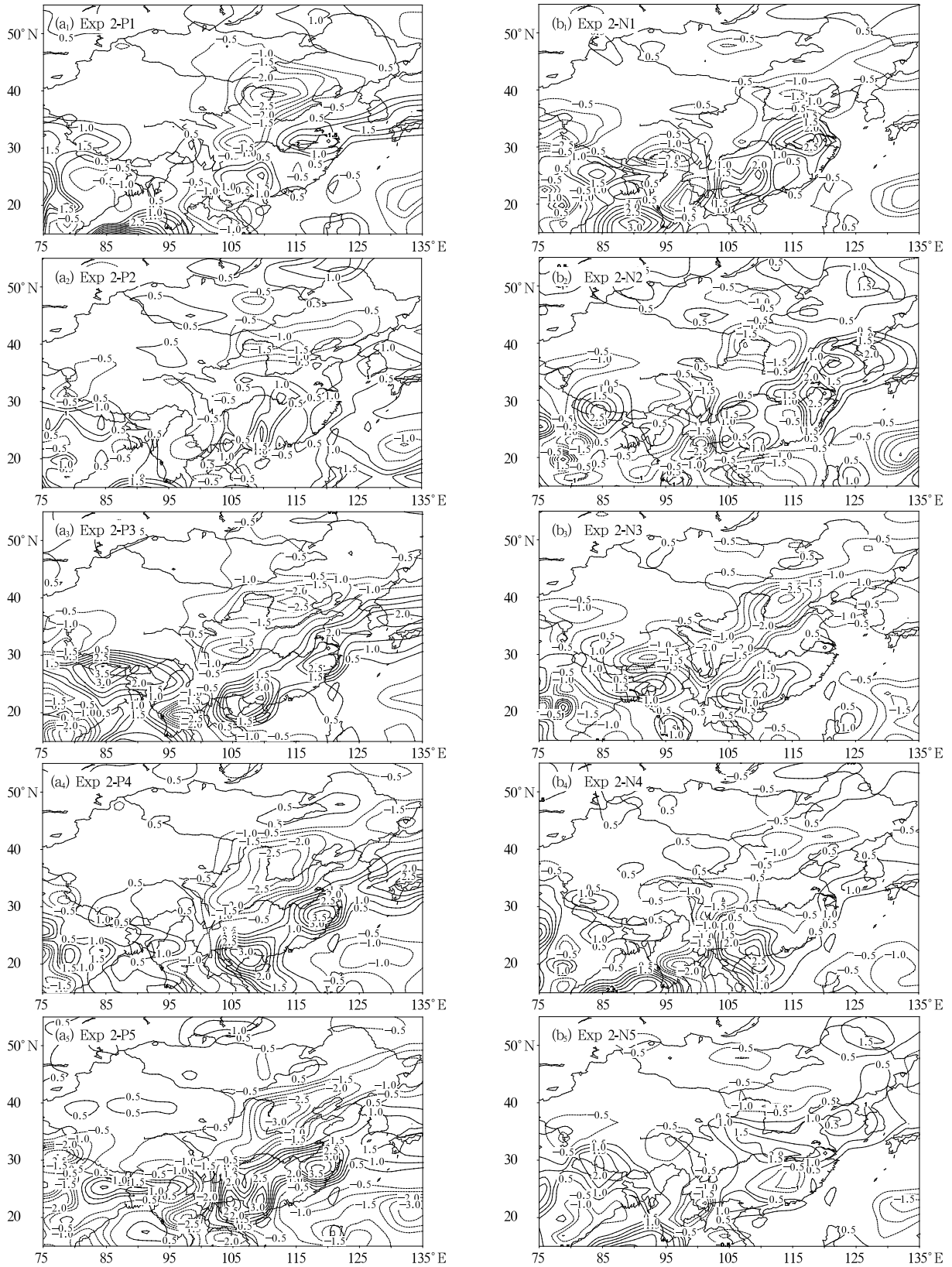


**Fig. 4.** The effect of various intensity P-SSTAs (left panels) and N-SSTAs (right panels) from September to June over the TEP on the precipitation anomalies ( $\text{mm day}^{-1}$ ) in June.

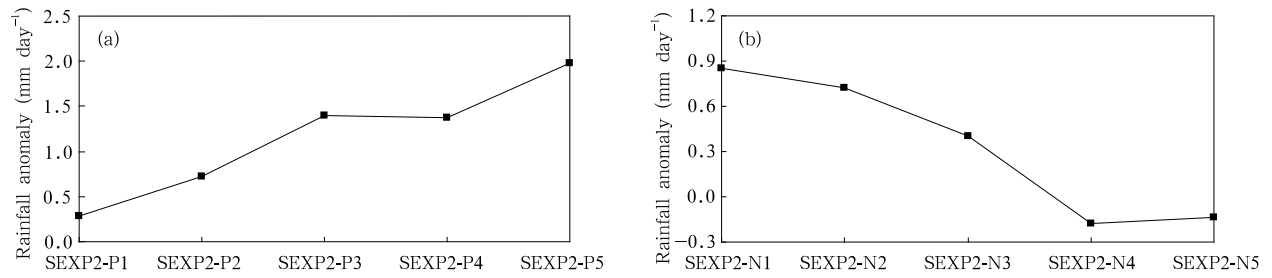


**Fig. 5.** The effects of various intensity P-SSTAs (a) and N-SSTAs (b) on the precipitation anomalies over the YRBS in June. The *x*-axis labels SEXP2-P1, ..., SEXP2-P5, and SEXP2-N1, ..., SEXP2-N5 show the name of each sensitivity experiment.

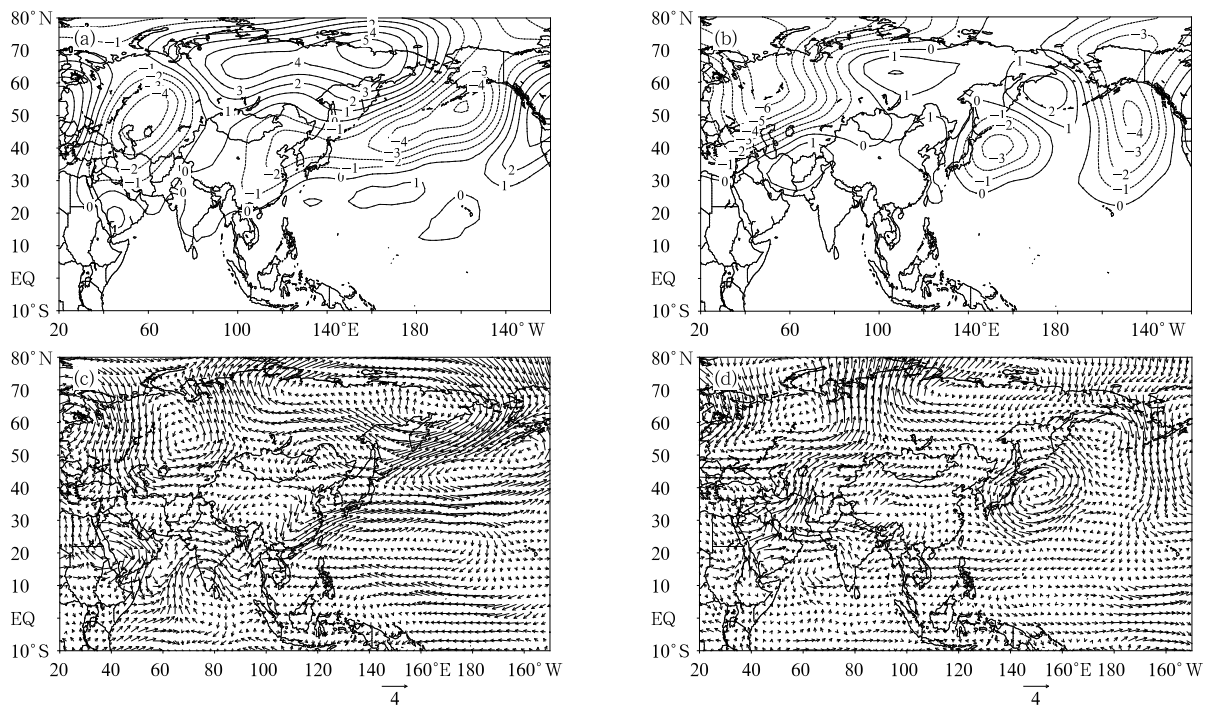


**Fig. 6.** The effects of SST anomalies over the TEP on Z500A (gpm) in (a) SEXP2-P3 and (b) SEXP2-N3, and on 850-hPa wind anomalies ( $\text{m s}^{-1}$ ) in (c) SEXP2-P3 and (d) SEXP2-N3 in June.

Z500A between the Baikal and the Okhotsk Sea is weaker than that in Fig. 6a. The anomalous low-level anticyclone circulation over the Philippine Sea is further westward compared with that in SEXP2-P3 and the strength of the anomalous low-level anticyclone circulation is far weaker than that in SEXP2-P3. Besides, there are no obvious anomalies southwesterly of current along South China. The area-averaged anomalous precipitation over the YRBS in SEXP2-N3 is  $0.3 \text{ mm day}^{-1}$ , which is much less than that in the SEXP2-P3 and no obvious precipitation anomalies can be found over other areas (Fig. 4). The simulations show that the response of the atmospheric

circulation anomalies and precipitation anomalies to La Niña events is not exactly opposite to that of El Niño events.

#### 4. Conclusions and discussion

Using the NCAR CAM3.0 model, we carried out several sensitive experiments to simulate the response of the atmosphere circulation and precipitation in June to SST anomalies over the equatorial eastern Pacific. According to the analyses of the simulation experiments, we draw the following conclusions:

- (1) The response of precipitation in the YRBS to

El Niño with different durations varies with the maximum amplitude of the precipitation anomalies appearing when the imposed duration is from November to next June, and the minimum appearing when the SST anomalies is only imposed in June. The anomalies of the precipitation are reduced when the duration of forcing SST anomaly is shortened, suggesting that the positive SST anomalies in the preceding autumn tend to cause significantly more rainfall in the YRBS. This is in agreement with previous diagnostic analysis results.

(2) The simulated precipitation anomalies over the YRBS are always obviously positive under strong or weak positive SST anomalies over the TEP. The intensity of the precipitation anomalies increases with increasing intensity of the SST anomalies in the experiments. The results of the simulations are consistent with the observations during the warm SST events, suggesting reasonable modeling results.

(3) When negative SST anomalies in the TEP are put into the model, the results are different from those of the diagnostic analysis of La Niña events. Negative precipitation anomalies in the YRBS could be reproduced only when the prescribed negative SST anomalies are strong enough.

Although the precipitation anomalies in South China are induced by many factors, the SST anomalies over the TEP seem to have played a critical role in causing the precipitation anomalies. Thus, studies of the influence of SST anomalies over the TEP on precipitation over the YRBS in June are of great importance to improve the understanding of monsoon rainfall variation. The AGCM models are forced by the observed or “perfectly predicted” SST and atmospheric models alone could be able to reproduce climate anomalies and capture the predictable portion of climate variations. The CAM3.0 used in this study properly simulated the response of precipitation anomalies over the YRBS in June to the SST anomalies over the TEP. However, present findings suggest that the coupled ocean-atmosphere processes are crucial in the monsoon regions where the atmospheric feedback on SST is important. It is necessary to consider the coupled atmosphere-ocean interaction

by using CGCMs (Coupled Ocean-atmosphere General Circulation Models) to confirm the conclusions in this study and improve the understanding of the effect of the SST anomalies over the TEP on the precipitation over the YRBS in June.

## REFERENCES

- Chang, C. P., P. Harr, and J. Ju, 2001: Possible role of Atlantic circulations on the weakening Indian monsoon rainfall-ENSO relationship. *J. Climate*, **14**(11), 376–380.
- Chen Hanshan, Sun Zhaobo, et al., 2002: Numerical experiments on the responses of the East Asian winter monsoon to autumn and winter SSTA. *Journal of Nanjing Institute of Meteorology*, **25**(6), 721–730. (in Chinese)
- Collins, W. D., P. J. Rasch, et al., 2004: Description of the NCAR Community Atmosphere Model (CAM3.0). Technical Report NCAR/TN-464+STR, National Center for Atmospheric Research, Boulder, Colorado, 210 pp.
- Dong Min, 1997: Validation study on the East Asian climate simulated by CCM2. *Acta Meteor. Sinica*, **55**(1), 692–702. (in Chinese)
- Kalnay, E., and Coauthors, 1996: The NCEP/NCAR 40-year reanalysis project. *Bull. Amer. Meteor. Soc.*, **77**(3), 437–471.
- Li Chongyin, Jia Xiaolong, and Dong Min, 2006: Numerical simulation and comparison study of the atmospheric intraseasonal oscillation. *Acta Meteor. Sinica*, **64**(4), 412–419. (in Chinese)
- Li Yan, Wang Yafei, and Wei Dong, 2007: Effects of anomalous SST in tropical Indian Ocean and Pacific Ocean on next June precipitation over the Yangtze River basin and area south of the basin. *Acta Meteor. Sinica*, **65**(3), 393–405. (in Chinese)
- Long-Range Weather Forecasting Group of Institute of Atmospheric Physics, 1978: *Impact of the Winter Pacific Sea Temperature on the precipitation in China*. Collection Journal of Institute of Atmospheric Physics, Chinese Academy of Sciences, No 6. Science Press. (in Chinese)
- Luo Shaohua, Jin Zuhui, and Chen Lieting, 1985: Correlation between sea surface temperature in Indian Ocean and South China Sea and summer precipitation over the mid-to-low reaches of the Yangtze

- River. *Chinese J. Atmos. Sci.*, **9**(3), 314–320. (in Chinese)
- Miao Qiuju, Xu Xiangde, and Zhang Xuejin, 2002: Characteristics of teleconnection wave train for circulation pattern of flood/drought in the middle and lower reaches of Yangtze River and sea surface temperature over equatorial East Pacific. *Acta Meteor. Sinica*, **60**(6), 688–697. (in Chinese)
- Namias, J., 1959: Recent seasonal interaction between North Pacific waters and the overlying atmospheric circulation. *J. Geophys. Res.*, **64**(2), 631–46.
- Rasmusson, E. M., and M. J. Wallace, 1983: Meteorological aspects of El Niño/Southern Oscillation. *Science*, **222**, 1195–1202.
- Su Zhixia, Lu Shihua, and Luo Siwei, 1999: The examinations and analysis of NCEP/NCAR 40 years global reanalysis data in China. *Plateau Meteorology*, **18**(2), 209–218. (in Chinese)
- Wang, Y., B. Wang, and Oh Jai-Ho, 2001: Impact of preceding El Niño on the East Asian summer atmosphere circulation. *J. Meteor. Soc. Japan*, **79**, 575–588.
- , and Y. Fujiyoshi, 2004: A case study on the relationship between a preceding La Niña event and the East Asian summer atmospheric circulation. *Acta Meteor. Sinica*, **18**(4), 387–396.
- Wang Yafei, 1992: Impact of blocking anticyclones in Eurasia in the rainy season (Meiyu/Baiu season). *J. Meteor. Soc. Japan*, **70**, 929–951. (in Chinese)
- Wang Zhongrui and Qian Yongfu, 2005: Influences of SSTA in Indian Ocean, South China Sea and Southeastern coastal region of China on Yangtze-Huaihe River valley precipitation of June and July. *Chinese J. Appl. Meteor.*, **16**(4), 527–538. (in Chinese)
- Wei Dong and Wang Yafei, 2006: Impact of the sea surface temperature anomaly of the east coast of Japan on the development of the Okhotsk high. *Acta Meteor. Sinica*, **64**(4), 518–526.
- Wu Guoxiong and Wang Jingfang, 1996: Comparison of the correlations of lower tropospheric circulation with tropical and extratropical sea surface temperature anomalies. *Acta Meteor. Sinica*, **54**(4), 385–397. (in Chinese)
- Xu Haiming, He Jinghai, and Dong Min, 2001: Interannual variability of the Meiyu onset and its association with North Atlantic oscillation and SSTA over North Atlantic. *Acta Meteor. Sinica*, **59**(6), 694–706. (in Chinese)
- Yuan Jiashuang, Zheng Qinglin, and Song Qingli, 2004: Numerical experiment of effects of persistent SSTA over northern Pacific Ocean on East Asian atmospheric circulation in early summer. *Journal of Nanjing Institute of Meteorology*, **27**(5), 623–631. (in Chinese)
- Yulaeva, K., and J. M. Wallace, 1994: The signature of ENSO in global temperature and precipitation field derived from the microwave sounding unit. *J. Climate*, **7**(11), 1719–1736.
- Zhang Qingyun and Tao Shiyan, 1998: Influence of Asian mid-high latitude circulation on East Asian summer precipitation. *Acta Meteor. Sinica*, **56**(2), 199–211. (in Chinese)